



## RESEARCH ARTICLES

### Rheology of Pharmaceutical Systems: Oscillatory and Steady Shear of Non-Newtonian Viscoelastic Liquids

GEORGE B. THURSTON\* and ALFRED MARTIN

Received December 8, 1977, from the Departments of Mechanical and Biomedical Engineering and the Drug Dynamics Institute, College of Pharmacy, University of Texas at Austin, Austin, TX 78712. Accepted for publication March 1, 1978.

**Abstract** □ A comparative analysis of oscillatory and steady shear rate measurements was made on carboxymethylcellulose solutions of two concentrations and two viscosity grades. In the oscillatory methods, the material is examined under nearly quiescent equilibrium conditions. Steady shear, conversely, produces large deformations and may yield false results, often interpreted as thixotropy, if the shear rate experiment is not conducted properly. Solutions of carboxymethylcellulose at concentrations ordinarily used in drug product formulations were examined by oscillatory and steady shear methods at low shear. Viscoelastic properties of pharmaceutical materials were measured using a newly developed oscillometric instrument. Mathematical expressions, formulated on the basis of a generalized Maxwell model for viscoelasticity and viscosity in steady shear, were correlated using these two rheological test methods. The results showed large increases in viscosity and relaxation time with increasing carboxymethylcellulose concentrations as well as with increasing molecular weights of the polymeric solute. The behavior of carboxymethylcellulose under both oscillatory and steady shear agreed with theory, linking the two methods of testing. Applications in pharmacy to this rheological analysis are presented. The present investigation attempted to bridge the gap between oscillatory and steady shear methods, demonstrating how both can find appropriate use in the analysis of non-Newtonian materials of pharmaceutical importance.

**Keyphrases** □ Carboxymethylcellulose—oscillatory and steady shear rate measurements compared, effect of concentration and viscosity grade □ Viscoelastic properties—carboxymethylcellulose, oscillatory and steady shear rate measurements compared, effect of concentration and viscosity grade □ Oscillatory measurements—compared to steady shear rate method, carboxymethylcellulose, effect of concentration and viscosity grade □ Steady shear rate measurements—compared to oscillatory method, carboxymethylcellulose, effect of concentration and viscosity grade

Polymer solutions such as carboxymethylcellulose dispersions and some pharmaceutical, food, and cosmetic products show shear thinning with increased shear rate. This phenomenon is characteristic of non-Newtonian liquids, which are referred to as pseudoplastic (1). When shear thinning is measured in a rotational viscometer of the concentric cylinder type or in the cone and plate configuration (2-4), the shear stress and shear rate often are

varied in a cyclic sequence. Starting from rest, the stress is measured with shear rate increasing, either continuously or stepwise at some prescribed rate, and then decreasing to rest.

With a Newtonian fluid, this procedure gives a graph of shear stress *versus* rate that is linear, the up and down curves being superimposed. With non-Newtonian fluid, the graph is generally concave toward the shear rate axis since the shear stress increases less rapidly than the shear rate. If the cyclic time is too short, the down curve may not coincide with the up curve. With the broader classification of thixotropic materials, the up and down curves may not coincide in any event (5).

#### BACKGROUND

In a solution of long chain polymer molecules, non-Newtonian behavior results from chain elongation induced by high shear stress and, at high polymer concentrations, may also involve ordering and disentanglement of the chains (1, 6). In colloids and suspensions, non-Newtonian behavior results from particle orientation, deformation, aggregation, disaggregation, and other structural modifications.

Davis (7) pointed out disadvantages of continuous, steady shear rheometry, principally the unavoidable disruption of the solid structure of a material during measurement. It is often impossible to separate the true rheological properties of complex materials from the instrumental effects when using a rotational, steady shear instrument (7). Schnaare *et al.* (8) also confronted these inherent problems.

An alternative approach to the rheology of non-Newtonian materials, that of viscoelastic measurements performed using small deformations including creep analysis, does not ordinarily disrupt particle aggregates in suspension, destroy the network of gels, or force entanglement effects in polymers. Creep tests have been used in pharmacy and cosmetic science (9-18). The measurement flexes the structures of the dispersions without destroying rheological characteristics. Other workers (19-21) described oscillatory equipment for the measurement of suspensions, gels, and blood in the unperturbed state or in the "rheological ground state," as Barry (9) termed it. By a mathematical transformation from the theory on linear viscoelasticity, oscillatory and creep measurements can be related (22) to one another.

Since the present work concerns a comparative analysis of oscillatory and steady shear rate measurements, it is necessary to make several distinctions in classifying these two conditions. First, oscillatory shear may be of either small or large amplitude. For small amplitude, the shear stress to shear rate relation is linear with a change in amplitude; therefore, a pure sinusoid of shear rate produces a pure sinusoid of shear stress at the same frequency. The material is thus examined under nearly quiescent, unperturbed, equilibrium conditions. For large amplitude, the state of the material may undergo some change because of finite deformations. The shear stress to shear rate relation may become nonlinear, and the sinusoidal waveforms take on some harmonic distortion.

Second, steady shear, unlike oscillatory shear, produces only large deformations, with the magnitude of deformation increasing at a constant rate with time. However, the growth rate of the deformation, *i.e.*, the shear rate, may be either low or high. Thus, continuous steady shear is incompatible with materials in the solid state since these materials can tolerate only limited deformations without destruction. Small oscillatory deformations can be employed for both solids and liquids, but steady shear is applicable only to liquids. Corresponding stress to strain rate relations probably are approached under conditions of very small shear rates using either steady shear measurements or oscillating measurements with the frequency of oscillation approaching zero. This limiting relationship is evaluated for the materials in the current investigation.

Within the framework of these concepts, the questions arise: Can thixotropy be meaningfully studied in steady shear? And, if conventional indications are found, is the material truly thixotropic? The fact that finite to infinite deformation of the material is involved in the test means that the material is a liquid, or it is a solid that has undergone disruption of the bulk material or slippage at the wall to permit deformation. Moreover, to achieve steady shear rate conditions, the shear rate must be maintained at a constant value for a time sufficiently long that equilibrium is attained and all recoverable effects from past deformational history are regained. The time needed for this effect is much longer than convenient for measurements on many materials. Measurements performed by instrumentation that continuously increases or decreases the shear rate may perpetuate the nonequilibrium condition and give a false indication of thixotropy. Careful attention is given to attainment of equilibrium in the work reported here.

In the present investigation, the behavior of the polymer, carboxymethylcellulose, in solutions of moderately high concentrations is examined using oscillatory shear measurements at low amplitudes and steady shear measurements. This comparison is done to examine limiting low shear rate–steady shear behavior with limiting low frequency oscillatory shear behavior. The extension to higher frequencies of oscillatory shear and higher rates of steady shear also is discussed. Mathematical expressions for viscoelasticity in oscillatory shear and for viscosity in steady shear are compared with the experimental results and provide a basis for the characterization of liquids under these two test methods.

## THEORETICAL

**Viscoelasticity in Oscillatory Shear**—The conceptual definition for viscoelastic behavior in oscillatory shear is represented in Fig. 1a. An idealized thin layer of material is subjected to an oscillatory driving force,  $F$ , resulting in a surface motion of velocity,  $V$ . The shear stress induced in the material,  $\tau$ , is directly proportional to  $F$ , while the shear rate,  $\dot{\gamma}$ , is proportional to  $V$ . If the frequency of this sinusoidal oscillation is  $(\omega/2\pi)$  Hz, then the shear rate and shear stress have the time dependencies:

$$\dot{\gamma} = \dot{\gamma}_M \cos(\omega t) \quad (\text{Eq. 1a})$$

$$\tau = \tau_M \cos(\omega t - \phi) \quad (\text{Eq. 1b})$$

where  $\phi$  is the phase difference between  $\tau$  and  $\dot{\gamma}$ . These phased sinusoids are shown in Fig. 1b. For a purely viscous material,  $\phi = 0$ ; for a purely elastic material,  $\phi = (\pi/2)$  rad. In the general viscoelastic case,  $\phi$  falls between these two limits. The shear rate and shear stress may be described using complex forms:

$$\dot{\gamma}^* = \dot{\gamma}_M \exp(i\omega t) \quad (\text{Eq. 2a})$$

$$\tau^* = \tau_M \exp(i\omega t - i\phi) \quad (\text{Eq. 2b})$$

the real parts of which are  $\dot{\gamma}$  and  $\tau$ . These are shown in a complex plane representation in Fig. 1c, where the phasors,  $\dot{\gamma}^*$  and  $\tau^*$ , rotate counterclockwise at an angular rotation rate,  $\omega$ . By forming the ratio of  $\tau^*$  to  $\dot{\gamma}^*$ , the complex coefficient of viscosity is defined. This ratio gives:

$$\eta^* = \tau^*/\dot{\gamma}^* \quad (\text{Eq. 3a})$$

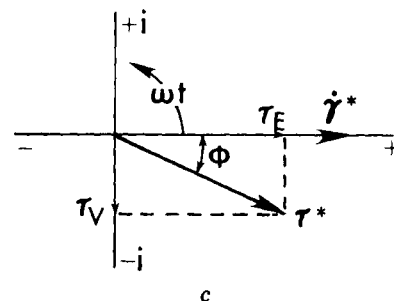
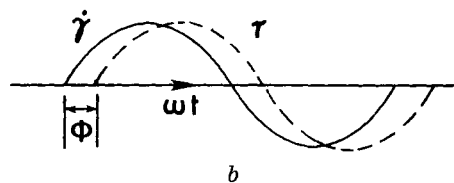
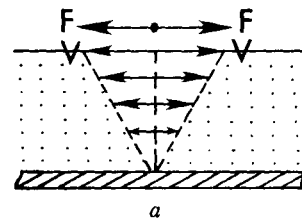


**Figure 1**—Viscoelastic behavior in oscillatory shear. A sample is subjected to oscillatory force,  $F$ , and velocity,  $V$ , at a radian frequency,  $\omega$ . The resulting shear stress,  $\tau$ , and the time rate of shear strain,  $\dot{\gamma}$ , differ in phase by the angle,  $\phi$ . These parameters are also shown in complex form by plotting in the complex plane.

$$\eta^* = (\tau_M/\dot{\gamma}_M) \exp(-i\phi) \quad (\text{Eq. 3b})$$

$$\eta^* = \eta \exp(-i\phi) \quad (\text{Eq. 3c})$$

where  $\eta$  is the magnitude and  $\phi$  is the phase of the viscoelastic modulus.

Equations 3a–3c may be resolved into real and imaginary terms, in which case the viscous and elastic parts are determined. In the diagram of the complex plane (Fig. 1), the complex shear stress,  $\tau^*$ , is shown resolved into that part in phase,  $\tau_V$ , with the shear rate,  $\dot{\gamma}^*$ , and that part in quadrature,  $\tau_E$ . These shear stresses are the viscous and elastic parts of  $\tau^*$ . Thus, the complex coefficient of viscosity is:

$$\eta^* = (\tau_V - i\tau_E)/\dot{\gamma}^* \quad (\text{Eq. 4a})$$

$$\eta^* = (\tau_M \cos \phi/\dot{\gamma}_M) - (i\tau_M \sin \phi/\dot{\gamma}_M) \quad (\text{Eq. 4b})$$

$$\eta^* = \eta_V - i\eta_E \quad (\text{Eq. 4c})$$

where  $\eta_V$  and  $\eta_E$  are the viscous and elastic parts of  $\eta^*$ . To interpret these parameters further, the viscous parts are associated with energy loss during the cyclic shearing while the elastic parts give cyclic storage and recovery of energy. This relation is seen by calculating the work done per unit volume of material during a portion,  $d(\omega t)$ , of the cycle:

$$(\text{work/volume}) = (\dot{\gamma}_M^2/\omega)(\eta_V \cos^2 \omega t + \eta_E \sin \omega t \cos \omega t) d(\omega t) \quad (\text{Eq. 5})$$

Averaging this work over one complete cycle gives the average power per unit value as:

$$(\text{power/volume}) = \eta_V(\dot{\gamma}_M^2/2) \quad (\text{Eq. 6})$$

which represents a nonrecoverable energy loss.

**Characteristic Behavior of Viscoelastic Liquids in Oscillatory Shear**—The viscoelastic behavior of liquids as seen by oscillatory shear measurements at small amplitudes of varying frequency can be analyzed using a generalized extension of the well-known Maxwell model (23)

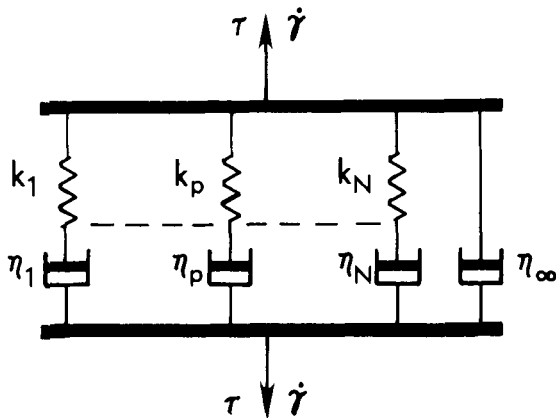


Figure 2—Generalized extension of the Maxwell model for a unit cube of material in shear.

shown in Fig. 2. The individual spring-dashpot combination in series is the element of Maxwell,  $N$  of these being shown in the model. The  $(N + 1)$  element is a dashpot alone, represented by  $\eta_\infty$ , this being the dissipative element controlling the viscoelasticity at infinite frequency.

At very low frequencies of excitation, the dashpot controls the mechanical behavior of the combination; at high frequencies, the strain becomes totally absorbed in the stretch and compression of the spring. The relaxation time,  $T_p$ , of the  $p$ th element serves as the "internal clock" that delineates the distinction between low and high frequencies according to whether  $(\omega T_p)$  is very much less than 1 or very much greater than 1, respectively. The contribution of the single element to the viscoelasticity of the assemblage is:

$$\eta_p^* = \eta_p / (1 + i\omega T_p) = \tau_p / \dot{\gamma}_p \quad (\text{Eq. 7})$$

where  $T_p$  is related to the damping factor and the spring constant,  $K_p$  (Fig. 2), by:

$$T_p = \eta_p / K_p \quad (\text{Eq. 8})$$

In this model, each Maxwell element is subject to the same shear rate,  $\dot{\gamma}$ , while shear stress,  $\tau_p$ , is additive for the stress,  $\tau$ , of the total system. Thus, the viscoelastic modulus for the complete assemblage is:

$$\eta^* = \sum_{p=1}^N \eta_p^* + \eta_\infty \quad (\text{Eq. 9})$$

Equation 9 can be rewritten in the form:

$$\eta^* = \eta_\infty + (\eta_0 - \eta_\infty) \sum_{p=1}^N H_p / (1 + i\omega T_p) \quad (\text{Eq. 10})$$

where:

$$\eta_0 = \sum_{p=1}^N \eta_p + \eta_\infty \quad (\text{Eq. 11})$$

and:

$$H_p = \eta_p / \sum_{p=1}^N \eta_p \quad (\text{Eq. 12})$$

Therefore:

$$\sum_{p=1}^N H_p = 1 \quad (\text{Eq. 13})$$

By taking the limits in Eq. 10 as  $\omega T_p \rightarrow 0$  and  $\omega T_p \rightarrow \infty$ ,  $\eta_0$  is the viscosity at zero frequency while  $\eta_\infty$  is the viscosity at infinite frequency, the elasticity vanishing at both limits.

The generalized Maxwell model can be considered an empirical model for a linear viscoelastic material. However, this model is produced exactly from two molecular theories for liquid solutions at low concentrations. One is for rigid, ellipsoidal macromolecules suspended in a viscous solvent (24, 25); the other is for flexible, linear polymer molecules (26). The more precise polymer chain theory including internal chain viscosity (27, 28) gives characteristics very similar to the Maxwell model (29-31). In going from dilute to concentrated polymer solutions, the theories are no longer strictly pertinent; however, the form of the model remains applicable (19). The Maxwell model can serve equally well as a basis for analysis of stress and strain rate relaxation experiments.

When a fluid containing  $N$  relaxation processes (i. e.,  $N$  Maxwell ele-

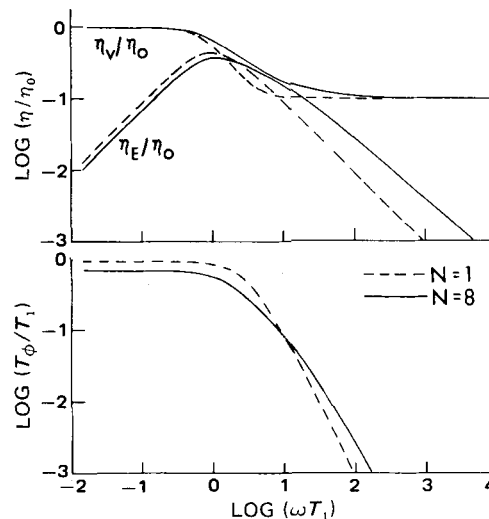


Figure 3—Frequency dependence of the viscous component,  $\eta_V$ , and the elastic component,  $\eta_E$ , of the viscoelasticity and the effective relaxation time,  $T_\phi$ .  $T_1$  is the longest relaxation time of the system. Calculations are for the generalized Maxwell model of Fig. 2, the dashed line curves being for  $N = 1$  and the solid line curves being for  $N = 8$ . Numerical parameters are given in the text.

ments) is subjected to oscillatory shear at a radian frequency,  $\omega$ , all processes contribute to the viscosity and elasticity but in differing amounts, depending on the individual values of  $\omega T_p$ . Only by examining  $\eta^*$  over a wide range of frequencies can some assessment be made of the extent of the characteristic relaxation times for a material. While, in principle, it is necessary to vary  $\omega$  from 0 to  $\infty$  to establish the complete relaxation spectra, the significant contribution of a single Maxwell element seen as  $\omega T_p$  ranges from 0.1 to 10. Thus, it is important to perform measurements in a particular frequency range to show the relaxation processes of interest.

Precise matching of theory and experiment to establish the  $N$  values of a relaxation time,  $T_p$ , for the generalized Maxwell model is difficult when several Maxwell elements are involved. However, a useful parameter that gives good insight into the relaxation spectrum is the "effective relaxation time," calculated as though there were a single element only. If the high frequency limiting viscosity,  $\eta_\infty$ , is known, this time is obtained from the phase of  $(\eta^* - \eta_\infty)$ . When  $\eta_\infty$  is not known, the phase of  $\eta^*$  alone can be used. The effective relaxation time is then:

$$T_\phi = (\tan \phi) / \omega \quad (\text{Eq. 14})$$

Applying this equation to the generalized model, using Eq. 9, gives:

$$T_\phi = \frac{\sum_{p=1}^N \frac{\eta_p T_p}{1 + (\omega T_p)^2}}{\left[ \sum_{p=1}^N \frac{\eta_p}{1 + (\omega T_p)^2} + \eta_\infty \right]} \quad (\text{Eq. 15})$$

This function is frequency dependent and approaches an upper limit, as  $\omega T_p \rightarrow 0$ , of:

$$T_{\phi,0} = \frac{\sum_{p=1}^N \eta_p T_p}{\left[ \sum_{p=1}^N \eta_p + \eta_\infty \right]} \quad (\text{Eq. 16})$$

The lower limit of this function is obtained for large values of  $\omega T_p$  as:

$$T_{\phi,\infty} = \frac{\sum_{p=1}^N (\eta_p / T_p)}{\left[ \sum_{p=1}^N \eta_p / T_p^2 + \eta_\infty \omega^2 \right]} \rightarrow 0 \text{ as } \omega T_p \rightarrow \infty \quad (\text{Eq. 17})$$

Thus, the function  $T_\phi$  generally falls in the range of the relaxation times of the contributing Maxwell elements.

The character of the frequency dependence of the viscous and elastic components of the complex coefficient of viscosity is shown in Fig. 3. Here, the ratios  $\eta_V/\eta_0$  and  $\eta_E/\eta_0$  are plotted versus  $\omega T_1$ , where  $T_1$  is the longest relaxation time for the system of relaxing elements. This plot is shown for a single relaxing element,  $N = 1$ , and for a multiple system,  $N = 8$ . The curves are computed using Eq. 10 with the following values:  $N = 1$  and  $H_1 = 1$ ; and  $N = 8$ ,  $T_p/T_1 = 1, 0.3, 0.1, 0.03, 0.01, 0.003, 0.001$ , and 0.0003, and  $H_p$  values are arbitrarily selected to be  $H_p = T_p / \sum_{p=1}^8 T_p$ .

**Characteristic Behavior of Liquids in Steady Shear**—The shear stress and shear rate for a liquid in steady flow can be related by:

$$\tau_s = [\eta_s(\dot{\gamma}_s)] \dot{\gamma}_s \quad (\text{Eq. 18})$$

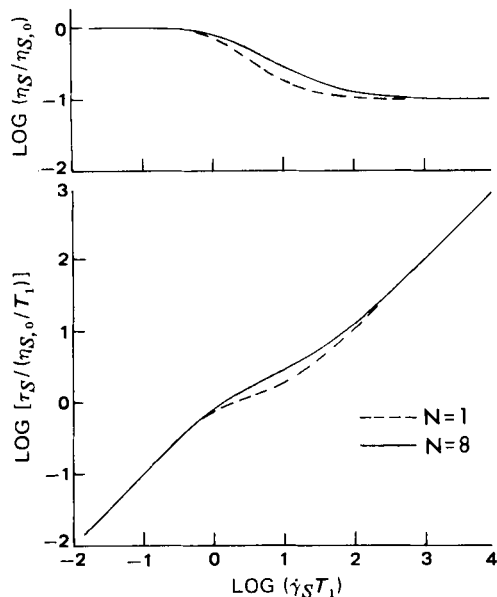


**Figure 4**—Steady shear rate dependence of viscosity,  $\eta_S$ , and shear stress,  $\tau_S$ , for the model of Fig. 2. The functions are calculated using Eqs. 24–26 and incorporating the same numerical factors used in Fig. 3 for the oscillatory flow case.

where  $\eta_S(\dot{\gamma}_S)$  is the shear rate dependent viscosity. For steady-state conditions and nonthixotropic materials, the  $\eta_S$  is independent of the past mechanical history of the sample and, thus, is the same when arrived at by either increasing or decreasing the shear rate. To make some determination of the time required to attain a steady-state flow condition, the stress is examined in the light of the generalized Maxwell model. The nonsteady-state solution for the contribution to the stress of a single Maxwell element is (32):

$$\tau_p = \int_{-\infty}^t (\eta_p/T_p) \exp[-(t-t')/T_p] \dot{\gamma}(t') dt' \quad (\text{Eq. 19})$$

When the shear rate,  $\dot{\gamma}(t')$ , is changed to a new value at time  $t_0$ , it can be shown by integration of Eq. 19 that the time factor  $[(t-t_0)/T_p]$  must become very large compared to 1 so that the stress contribution,  $\tau_p$ , becomes equal to  $\eta_p \dot{\gamma}$  as is necessary for Eq. 18 to be valid. Thus, in performing steady shear measurements on systems where the longest relaxation time is the order of seconds, a waiting period on the order of minutes may be necessary to achieve an equilibrium steady shear measurement.

The shear rate dependent viscosity is generally a decreasing function of shear rate once the shear rate exceeds some initial value below which  $\eta_S$  is constant. For polymers, this critical shear rate is nearly equal in magnitude to the radian frequency at which the viscoelasticity begins its dispersion (33–35). This characteristic shear rate dependence is derivable from molecular theories for dilute solutions of rigid ellipsoidal molecules (25) and dumbbell shapes (36, 37) and for linear polymer chains with internal viscosity (27, 28). A number of constitutive equations also exhibiting this character were developed (32).

The similarities observed between  $\eta^*(\omega)$  and  $\eta_S(\dot{\gamma}_S)$  suggest that the same fluid structural mechanisms are responsible for both functions in liquids, particularly at low frequencies and low shear rates. The generalized Maxwell model may serve as a basis for describing this similarity. For small oscillatory shear in the limit as  $\omega \rightarrow 0$ :

$$\eta^*|_{\omega \rightarrow 0} = \eta_0 = \eta_\infty + \sum_{p=1}^N \eta_p \quad (\text{Eq. 20})$$

This limiting condition can be assumed to coincide with the steady shear result as  $\dot{\gamma}_S \rightarrow 0$ , in which case:

$$\eta_S|_{\dot{\gamma}_S \rightarrow 0} = \eta_{S,0} = \eta_\infty + \sum_{p=1}^N \eta_{S,p}(0) \quad (\text{Eq. 21})$$

where  $\eta_{S,p}(0)$  is the limiting value of the damping factor for the Maxwell element as  $\dot{\gamma}_S \rightarrow 0$  and, under this condition, is the same as  $\eta_p$ .

For polymer solutions, there is a cutoff of relaxation processes with increasing steady shear rate (38, 39). The processes having the longest relaxation times are the first to be suppressed. In terms of the generalized Maxwell model, this condition means that the  $\eta_p$  values are dependent

upon the steady shear rate,  $\dot{\gamma}_S$ , and may be specified as  $\eta_{S,p}(\dot{\gamma}_S)$ . The character of this dependence may be written as:

$$\eta_{S,p}(\dot{\gamma}_S) = \eta_{S,p}(0) F(\dot{\gamma}_S T_p) \quad (\text{Eq. 22})$$

where the product  $\dot{\gamma}_S T_p$  is dimensionless and  $T_p$  is the relaxation time of the  $p$ th Maxwell element.

Under these conditions, the model gives the steady flow viscosity as:

$$\eta_S(\dot{\gamma}_S) = \eta_\infty + \sum_{p=1}^N \eta_{S,p}(\dot{\gamma}_S) \quad (\text{Eq. 23})$$

Equation 23 may be put into a form similar to Eq. 10:

$$\eta_S(\dot{\gamma}_S) = \eta_\infty + (\eta_{S,0} - \eta_\infty) \sum_{p=1}^N B_p F(\dot{\gamma}_S T_p) \quad (\text{Eq. 24})$$

where:

$$B_p = \eta_{S,p}(0) / \sum_{p=1}^N \eta_{S,p}(0) \quad (\text{Eq. 25})$$

and  $B_p = H_p$  under the assumption of the common model for oscillatory flow at low frequency and steady flow at low shear rates.

There are numerous possible functions  $F(\dot{\gamma}_S T_p)$  with the generally desired properties that will truncate a relaxation process. Several such functions have appeared in the rheological literature in other contexts to describe the shear rate dependence of steady flow viscosity. The function  $[1/(1+X^2)]$  was used by Lamb (40) for lubricating oils, while the square root of this function appeared in the derivation of Williams (41) for polymer solutions using an elastic dumbbell model. Tanner and Simmons (38) obtained the function  $[1 - (1+1/X) \exp(-1/X)]$  in an analysis of breakage of polymer entanglements.

The character of  $\eta_S(\dot{\gamma}_S)$  from Eq. 24 is illustrated using:

$$F(\dot{\gamma}_S T_p) = 1/[1 + (\dot{\gamma}_S T_p)^2]^{1/2} \quad (\text{Eq. 26})$$

This relationship is shown in Fig. 4 where  $(\eta_S/\eta_{S,0})$  is plotted versus  $\dot{\gamma}_S T_p$ . The curves are for the same series of Maxwell models as shown for the oscillatory flow in Fig. 3. Also in Fig. 4 are curves showing a factor proportional to shear stress plotted versus shear rate for the same two cases.

**Measurement of Viscoelasticity**—The basis for measurement of the complex coefficient of viscosity is from the analysis of the pressure to volume flow relation in a rigid straight tube of circular cross section. The theory for this oscillatory flow of viscoelastic liquids was developed by Thurston (42) and has been tested thoroughly in measurements (43). The pressure and volume flow are sinusoidal and follow a time variation in the complex plane that is proportional to  $\exp(i\omega t)$ . With a volume flow of  $U$  and a complex pressure drop per unit length of tube of  $P^*$ , this pressure can be resolved into component  $P'$  in phase with the flow and  $P''$  in quadrature with the flow. Then:

$$P^* = P' + iP'' \quad (\text{Eq. 27})$$

The relation between  $P^*$ ,  $U$ , the tube radius  $a$ , and the viscous and elastic components,  $\eta_V$  and  $\eta_E$ , is particularly simple in small tubes at low frequencies when the dimensionless parameter:

$$a[\rho\omega/|\eta^*|]^{1/2} < 1 \quad (\text{Eq. 28})$$

where  $\rho$  is the fluid density. Under this condition, the components of viscoelastic modulus are given by:

$$\eta_V = (\pi a^4/8)(P'/U) \quad (\text{Eq. 29})$$

$$\eta_E = (\pi a^4/8)[(4\rho\omega/3\pi a^2) - (P''/U)] \quad (\text{Eq. 30})$$

The complex shear stress at the tube wall is also determined from the pressure and flow:

$$\tau_{\omega}^* = (a/2)P^* - (i\omega\rho/2\pi a)U \quad (\text{Eq. 31})$$

With Eq. 31, the shear rate at the tube wall is given by:

$$\dot{\gamma}_\omega = \tau_{\omega}^*/\eta^* \quad (\text{Eq. 32})$$

## EXPERIMENTAL

Measurements of the pressure and volume flow were obtained using an apparatus designed by Thurston (44) (Fig. 5). The oscillatory flow in this apparatus is developed by a piston-like driver, the motion of which is monitored by a velocity-sensitive transducer attached to the drive shaft. The product of this shaft velocity times the effective area of the driver gives the instantaneous representation of the flow,  $U$ . This flow is

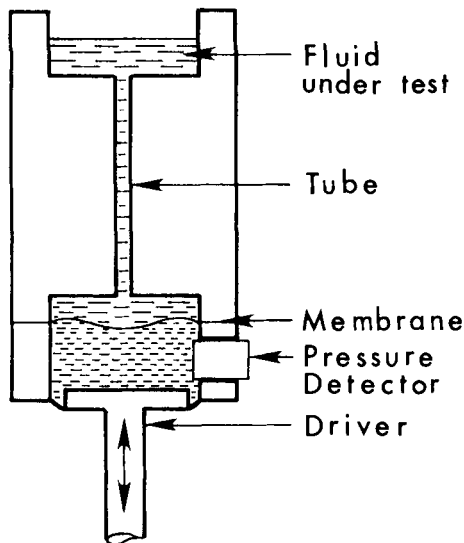


Figure 5—Schematic drawing of apparatus for measuring oscillatory flow properties of a viscoelastic fluid in a small tube having a circular cross section (42).

transmitted through a coupling fluid, water, through a flexible separating membrane, to the fluid under test that fills the tube. The pressure developed across the tube is monitored by the pressure detector,  $P$ .

Small corrections to the measured pressure and flow are made to compensate for residual chamber impedances. The electrical signals representing the pressure and volume flow are analyzed to obtain the desired in-phase and quadrature components of the pressure. The tube is always selected for the test fluid such that Eq. 28 is valid. Furthermore, the tube length is usually greater than the tube radius by a factor of 50 or more, thereby minimizing the effects of small tube length corrections. The complete system is calibrated using water as a viscosity standard.

The viscoelastic properties of the carboxymethylcellulose solutions were measured in the oscillatory flow frequency range of 0.05–100 Hz. In all cases, the amplitude of the oscillatory shear rate at the wall of the containing tube was held sufficiently low so that no nonlinear effects were evident. This condition was checked for each case by first increasing the amplitude to establish that the sample  $\eta^*$  remained unchanged. All measurements were made at 24°.

**Measurement in Steady Flow**—Steady flow of non-Newtonian liquids ordinarily is measured in a rotational viscometer, an instrument that continuously shears the material at various rates within the annular space between a stationary cup and a rotating inner cylinder or bob.

Measurements of steady shear were made by use of the steady shear rotational instrument<sup>1</sup>, which was provided with both coaxial cylinder and plate and cone sensor systems. Only the coaxial cylinder attachment was used. The instrument allows measurement of Newtonian and non-Newtonian materials over a shear rate range of  $10^{-3}$ – $4 \times 10^4$   $\text{sec}^{-1}$  and shear stress range of 2– $10^7$  dynes/cm<sup>2</sup>. Viscosity from 0.02 to  $10^8$  poises can be measured. Temperature was controlled in the annular space of the concentric cylinders by means of a constant-temperature circulator adjusted to  $25 \pm 0.1^\circ$ . Data were collected manually, point by point, with the rheometer or obtained automatically with a programmer attachment, and the up-and-down curves of shear stress versus shear rate were plotted continuously using an  $x$ - $y$  recorder.

The instrument was programmed to provide speeds for rotation of the inner cylinder between 1 and 100 rpm. The speed was changed automatically at 10, 25, 50, 75, 100, 150, 200, 250, 300, and 400 rpm/min, depending on the dial setting chosen.

In preparation for measurement, a sample of the solution was poured into the outer cylinder using the proper rotating inner cylinder (rotor) found in preliminary tests to provide a suitable rheogram within the specified viscosity range. The sample was allowed to stand undisturbed in the cylinder (covered with plastic film to prevent evaporation) for approximately 30 min. The constant-temperature control maintained the sample at  $25 \pm 0.1^\circ$  during the experiment.

For the concentric cylinder system, shear rate,  $\dot{\gamma}_S$   $\text{sec}^{-1}$ , is obtained

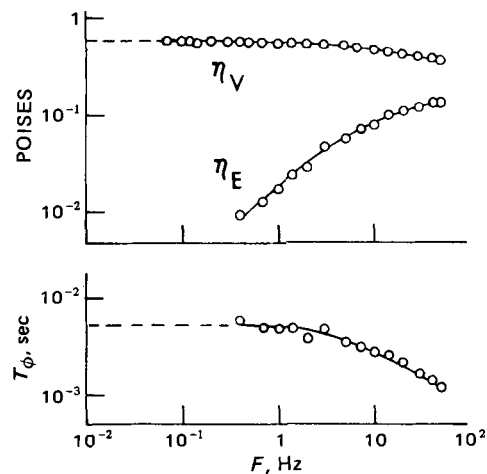


Figure 6—Viscoelastic properties of 1% carboxymethylcellulose solution (medium viscosity grade) under oscillatory shear flow. The viscosity,  $\eta_V$ , and elasticity,  $\eta_E$ , are defined in Eq. 4;  $T_\phi$  is the effective relaxation time defined in Eqs. 14–17.

from the rotor speed and an appropriate shear rate factor,  $M$ . Shear stress,  $\tau$ , depends on the scale value,  $S$ . It is obtained by multiplying  $S$  by an instrumental shear stress factor,  $A$ , to yield shear stress in dynes per square centimeter. The viscosity of a sample (in poises) at various shear rates is obtained from the scale reading,  $S$ , the revolutions per minute setting,  $n$ , and the instrumental constant,  $G = 100A/M$ , which varies depending on the measuring head and sensor used:

$$\eta = (G)(S/n) \quad (\text{Eq. 33})$$

The rotational instrument was supplied with calibration certificates giving the values of  $A$  and  $M$  for the various sensor systems, based upon the geometry of the measuring parts. These constants were checked using glycerin–water mixtures of established viscosities (45) and standard viscosity samples<sup>2</sup>. The results using both the instrument calibration values and the standard viscosity samples gave viscosity values that differed by less than 2% for the significant portions of the curve. Care must be taken not to make measurements below scale values of  $S = 10$  or 15 where errors in results may become large.

To correlate oscillatory results with steady shear values, it is necessary to examine the steady shear data at low shear rates. The rotational instrument is not ordinarily capable of accurate results below shear rate values of 1–10  $\text{sec}^{-1}$  and shear stress values below  $10^2$  dynes/cm<sup>2</sup>.

A Couette instrument<sup>3</sup>, giving accurate values at shear rates as low as 0.1  $\text{sec}^{-1}$ , was used to extend the measurement range. By combining the data from the two instruments, the shear stress to shear rate characteristics were revealed over a range of four decades.

The same four samples used in the oscillatory analysis were measured in steady shear flow. The next section describes the materials used in this investigation. In each case, the shear stress versus shear rate was measured with the rotational viscometer using two modes of measurement: (a) by automatic stepping of the shear rate in which the sample was cycled from a low shear rate to a high one and then back to a low one, and (b) by a manual method in which the time between measurements was lengthened to try to assure equilibrium conditions (see discussion following Eq. 19). The rotational measurements were carried out at 25°. Similarly, manual equilibrium measurements were made with the Couette viscometer at low shear rates and at 24°.

**Sample Preparation**—Carboxymethylcellulose sodium<sup>4</sup>, high viscosity food grade and medium viscosity grade powders, was obtained in sealed containers. The high viscosity food grade had a weight average molecular weight<sup>5</sup> of 700,000 and a degree of polymerization<sup>5</sup> of 3200. The medium food grade had a molecular weight<sup>5</sup> of 250,000 and a degree of polymerization<sup>5</sup> of 1100.

The polymer solutions were prepared by a standard procedure. Sam-

<sup>2</sup> Brookfield Engineering Laboratories, Houghton, MA 02072.

<sup>3</sup> Designed by G. B. Thurston.

<sup>4</sup> Cellulose Gum, Hercules Inc., Wilmington, Del.

<sup>5</sup> Values provided by the manufacturer.

<sup>1</sup> Haake Rotovisco, RV2, Haake Instruments, Saddle Brook, NJ 07662.

**Table I—Measurement Ranges and Rheological Limiting Values**

Sample <sup>a</sup>	Frequency Range, Hz	Shear Rate Range, sec <sup>-1</sup>	$\eta_{V,0}$ , poises	$T_{\phi,0}$ , sec
I	0.1–50	2.0–81	0.57	0.006
II	0.1–50	0.1–22	5.7	~0.17
III	0.05–50	0.02–23	12.3	>0.8
IV	0.07–100	0.007–4	>>162.0	>>1.5

<sup>a</sup> I = medium viscosity 1% solution, II = medium viscosity 2% solution, III = high viscosity 1% solution, and IV = high viscosity 2% solution.

**Table II—Experimental Conditions and Results for the Four Samples of Carboxymethylcellulose Tested<sup>a</sup>**

Sample <sup>b</sup>	Automated Total Average Time for Up and Down Plot, min	Manual Rate Average Time at Each Point, min	Manual Total Average Time for Up and Down Plot, min	$\eta_{S,0}$ , poises
I	31	5	59	0.58
II	22	6	50	5.6
III	30	6	61	13.4
IV	41	4	50	>>80

<sup>a</sup> For all four samples, the automated increment rate (rate of change) was 10 rpm/min and the Couette manual rate was 30 sec/point. <sup>b</sup> The sample numbers are the same as in Table I.

ples were placed in a continuous air-flow oven at 55° and dried to constant weight. The loss in weight, assumed to be due to moisture, was thus accounted for; this procedure permitted calculation of the amount undried to be used in preparing the carboxymethylcellulose solutions. Solutions of high and medium grades were prepared in concentrations of 1.0 and 2.0% in water containing a preservative mixture consisting of 0.1 g of propylparaben and 0.1 g of methylparaben/100 g of solution.

The solutions were made in 300-g quantities using warm water and a propeller blade stirrer. The samples were stored at room temperature in wide-mouth glass containers with plastic screw caps and liners. Preliminary work without parabens present showed that preservation was required for product viscosity to remain constant over time. Later results showed that, at the concentration of preservatives used, viscosities began to decrease after 4 months.

**Oscillatory Shear Results**—The results of oscillatory shear measurements on the carboxymethylcellulose medium grade 1 and 2% and high viscosity grade 1 and 2% are shown in Figs. 6–9. In each figure, the viscoelasticity is given in terms of  $\eta_V$  and  $\eta_E$  (see Eqs. 3c and 4c). The effective relaxation time,  $T_{\phi}$ , is also given.

The character of the theoretical frequency–response curves of Fig. 3 is clearly seen in the experimental curves (Figs. 6–9). However, the frequency range of the experimental data is not sufficient to reveal both the low and high frequency limits; with the high viscosity gums in 2% solution (Fig. 9), neither limit was seen. Table I summarizes the measurement conditions and low frequency limiting values. With increasing concentration, the breadth of the relaxation spectrum increased. Furthermore,  $\eta_{V,0}$  and  $T_{\phi,0}$  increased. These effects confirm that the polymer molecules in the solutions are highly interactive.

**Steady Shear Results**—The results of the steady shear measurements are shown in Figs. 10 and 11.

Table II summarizes the measurement conditions and the results obtained. The data in columns 2–5 were obtained using the commercial rotational viscometer. The values in column 6 are for the Couette instrument. The automated and manual results were identical for the medium viscosity samples but not for the high viscosity samples. Thus, because of the longer relaxation times of the higher molecular weight

samples, the automated measurements were nonequilibrium values and could be misinterpreted as indicative of thixotropic behavior. But the longer manual waiting period between measurement results in equilibrium and removes this artifact.

Comparison of the experimental curves (Figs. 10 and 11) with the theoretical curves of Fig. 4 shows that the general behavior is in agreement with the theory. With the exception of the high viscosity 2% sample, the low shear rate-limiting condition ( $\dot{\gamma}_S T_1 > 1$ ) was achieved, but the high shear rate limit was not.

**Oscillatory and Steady Shear Correlations**—Comparison of the low frequency limiting value of  $\eta_{V,0}$  and the low shear rate value of  $\eta_{S,0}$  (Tables I and II) shows that they do indeed approach the same limit. This result is in agreement with the postulate under *Theoretical*, in which the generalized Maxwell model is applied to both steady and oscillatory flow (Eqs. 20 and 21).

A second point for comparison is the relaxation times. Figures 10 and 11 show that the range of the relaxation spectrum becomes enlarged with both increasing concentration and increasing molecular weight. This result is consistent with that found in the oscillatory cases. A quantitative comparison can be made on the basis of estimates of the longest, dominant relaxation time for the sample. As shown by the sample theoretical curves of Fig. 3, when the shear stress has deviated approximately 15% from the linear extrapolated value, the product  $\dot{\gamma}_S T_1 \approx 1$ . While the deviation is clearly a function of the polydispersity of the sample's relaxation spectrum, this value can be used as a basis for estimation.

Similarly, one can use a condition on the  $\eta_V$  for which  $\eta_V$  has decreased 30% from its limiting value, and this occurs when  $\omega T_1 \approx 1$ . Table III summarizes this comparison. The data range for the high viscosity 2% Sample IV was not sufficient for this procedure. Table III lists the critical shear rate corresponding to the 15% deviation of  $\tau_S$ , the critical frequency

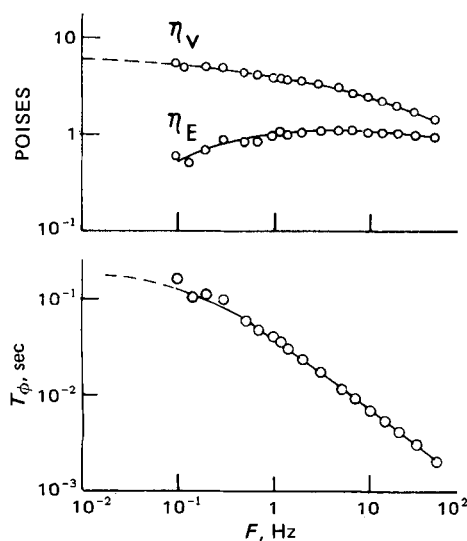


**Figure 7**—Viscoelastic properties of 2% carboxymethylcellulose solution (medium viscosity grade). See Fig. 6 for explanation of symbols.

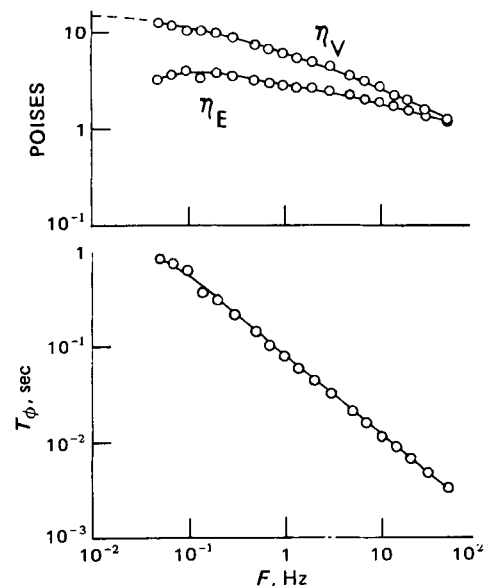


**Figure 8**—Viscoelastic properties of 1% carboxymethylcellulose solution (high viscosity grade). See Fig. 6 for explanation of symbols.

**Table III—Comparison of Relaxation Times for Steady and Oscillatory Flow**

Sample <sup>a</sup>	Critical Shear Rate, $\dot{\gamma}_S$ , sec <sup>-1</sup>	Critical Frequency, Hz	$T_1$ , Steady, sec	$T_1$ , Oscillatory, sec
I	80	30	0.012	0.0053
II	4.6	1.2	0.22	0.133
III	2.0	0.25	0.5	0.64

<sup>a</sup> The sample numbers are the same as in Table I.

corresponding to the 30% deviation of  $\eta_V$ , and the terminal relaxation time,  $T_1$ , calculated from these critical values.

The degree of agreement between the relaxation times is reasonable considering the method of estimation used. Complete characterization via the generalized Maxwell model requires specification of all the  $T_p$  and weighting factors,  $H_p$  (see Eqs. 10–13), as well as the zero frequency and high frequency limits,  $\eta_0$  and  $\eta_\infty$ . Before  $T_1$  can be evaluated exactly, it is necessary to have all of the spectral information. Thus, the  $T_1$  estimates will improve with increased information on the relaxation spectrum. Also, while the  $T_\phi$  values have an exact definition, they cannot be related exactly to the  $T_1$  values without additional information (Eqs. 14–16). These limitations on exact interpretations are common to all methods of rheological characterization when one seeks to describe multirelaxational molecular systems by means of only a few numerical factors.

**Applications in Pharmacy**—Added insights are gained through the analysis of the viscoelastic properties,  $\eta_V$  and  $\eta_E$ . For 1 and 2% medium viscosity carboxymethylcellulose,  $\eta_V$  remained relatively constant over a wide frequency range;  $\eta_E$ , on the other hand, passed through a maximum. The phase angle,  $\phi$ , tended to rise, whereas the “effective relaxation time,”  $T_\phi$ , decreased in a linear manner. These phenomena are characteristic of solutions of long chain molecules and can be used to characterize samples of carboxymethylcellulose and similar polymeric materials found in pharmacy. The values of  $\eta_V$ ,  $\eta_E$ ,  $\eta$ ,  $\phi$ , and  $T_\phi$  can serve as raw material specifications for commercial lots of suspending agents entering the manufacturing plant. They can also be used to adjust product characteristics in the research and design of new drug and cosmetic formulations. Studies on the rheology of disperse systems were reviewed by Barry (9). New approaches include the use of creep and oscillatory methods for the analysis of pharmaceutical and cosmetic products.

The present investigation attempts to bridge the gap between oscillatory and steady shear methods. The application of steady shear methods for anything more than estimations of flow properties of products in practical use was criticized (5, 7). It was thought that a product

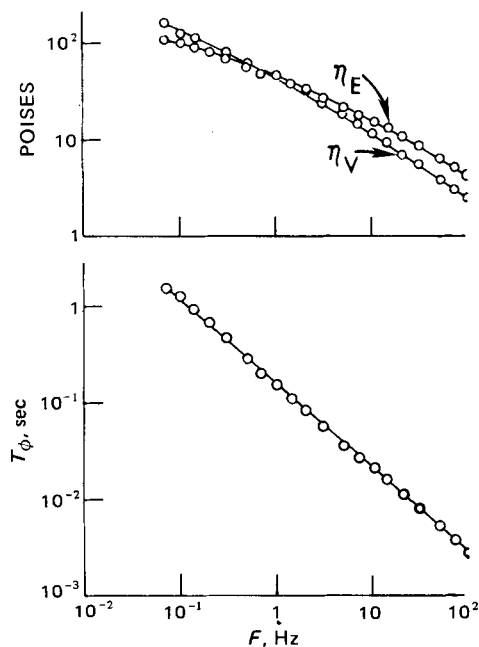


**Figure 9**—Viscoelastic properties of 2% carboxymethylcellulose solution (high viscosity grade). See Fig. 6 for explanation of symbols.

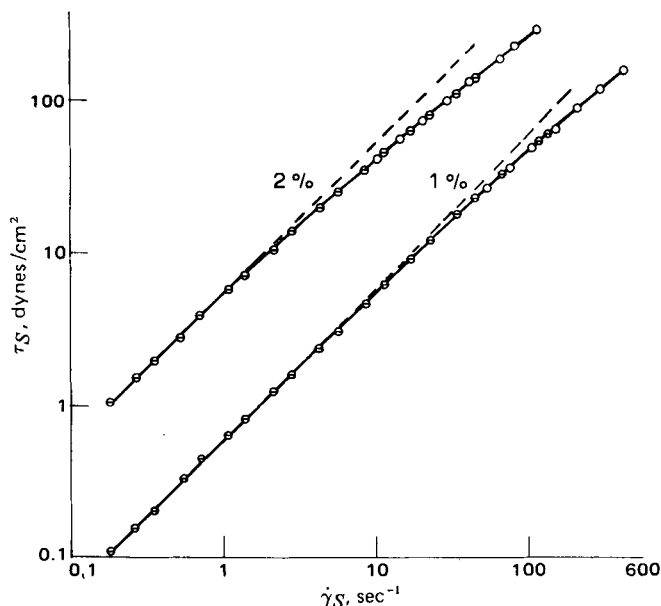


**Figure 10**—Steady shear stress versus shear rate for 1 and 2% carboxymethylcellulose solutions (medium viscosity grade) in the rotational viscometer. Dashed lines show the deviation from linearity at high shear. Open circles are commercial viscometer values; cross-line circles are values obtained with the Couette instrument.

under rotational shear is no longer in its “rheological ground state,” its structure being so severely perturbed by the shearing action that fundamental characteristics of the material cannot be studied (5, 7). Although rotational viscometry, mainly of the cone and plate geometry (7), was used, the application of creep or oscillatory experiments was suggested to obtain basic understanding of rheological materials, for the testing of theories of molecular structure, and for studying effects of formulation changes, storage temperature, and use characteristics of ointments, creams, and lotions.

For the carboxymethylcellulose solutions, the present study has demonstrated how a joint study of oscillatory perturbation together with steady shear in a rotational instrument can provide insight into the nature of viscoelastic materials used in pharmacy. Similar investigations should be carried out for cosmetics, paints, plastics, and other industrial materials. Through such work, a better understanding of the materials and

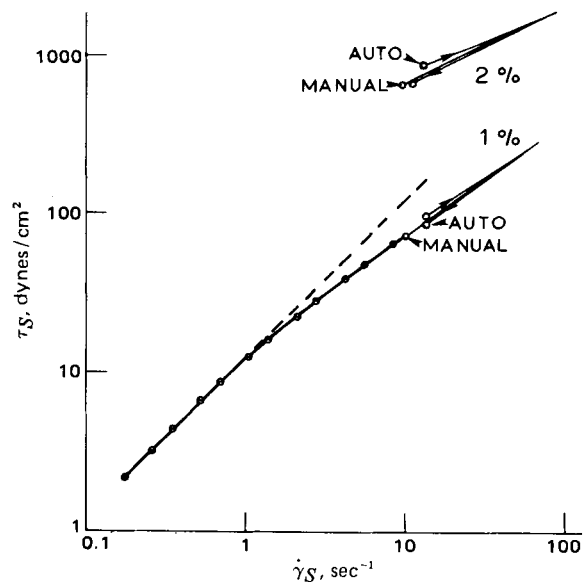


**Figure 11**—Steady shear stress versus shear rate for 1 and 2% carboxymethylcellulose solutions (high viscosity grade). The results for both automatic and manual operations of the commercial rotational viscometer are shown. Open circles are commercial viscometer values; cross-line circles are values obtained using the Couette instrument.

test methods of rheology can be obtained so that one may intelligently employ the equipment most appropriate to the preparation whose rheological properties are under investigation. Carboxymethylcellulose is a relatively well behaved material, a polymeric solution of practical use in pharmacy, and shows interesting rheological properties. It remains to be determined whether the analysis used here can be extended to gels, emulsions, and suspensions.

This analytic method offers a theoretical approach to steady shear measurements of non-Newtonian materials. It provides the possibility for a more fundamental understanding of results obtained with rotational and cone-plate steady shear viscometers. An evident suggestion uncovered by the work is that commercial rheometers should be designed to operate in the range of low shear rates of approximately 0.1 or 0.01 sec<sup>-1</sup> where results correspond more nearly to oscillatory findings and thus provide a knowledge of rheological structures in the ground state. Then, proceeding from low to high shear rates, of which commercial instruments are quite capable, will provide useful data on how the unperturbed gel, emulsion droplet, or suspension structure is altered by processing, packaging, and actual use. In this manner, the gap between theoretical and practical knowledge of rheology can be bridged and advances in applied and structural rheology can be accelerated. It is hoped that this study will help join two important aspects of rheology, nondestructive oscillation of products vis à vis deformation at high shear in rotating instruments, and will provide theoretical and experimental approaches to this end.

The next study will extend the method to the characterization of thixotropic materials.

### REFERENCES

- (1) "Remington's Pharmaceutical Sciences," 15th ed., Mack Publishing Co., Easton, Pa., 1970, pp. 354, 356.
- (2) J. C. Boylan, *Bull. Parenteral Drug Assoc.*, **19**, 98 (1965).
- (3) J. C. Boylan, *J. Pharm. Sci.*, **55**, 710 (1966).
- (4) *Ibid.*, **56**, 1164 (1967).
- (5) G. W. S. Blair, "Elementary Rheology," Academic, New York, N.Y., 1969.
- (6) W. W. Graessley, "Advances in Polymer Science," vol. 16, Springer-Verlag, New York, N.Y., 1974, pp. 1-179.
- (7) S. S. Davis, *Pharm. Acta Helv.*, **40**, 161 (1974).
- (8) R. L. Schnaare, R. M. Sheikh, P. J. Niebergall, and E. T. Sugita, *J. Pharm. Sci.*, **65**, 1385 (1976).
- (9) B. W. Barry, in "Advances in Pharmaceutical Sciences," vol. 4, H. S. Bean, A. H. Beckett, and J. E. Carless, Eds., Academic, New York, N.Y., 1975, p. 1.
- (10) W. H. Bauer and E. A. Collins, in "Rheology, Theory and Applications," vol. 4, F. R. Eirich, Ed., Academic, New York, N.Y., 1967, p. 425.
- (11) S. S. Davis, *J. Pharm. Sci.*, **58**, 412 (1969).
- (12) *Ibid.*, **60**, 1351 (1971).
- (13) S. S. Davis, *J. Sci. Instrum.*, **1**, Series 2, 933 (1968).

- (14) *Ibid.*, **2**, Series 2, 102 (1969).
- (15) S. S. Davis, *J. Text. Stud.*, **4**, 15 (1973).
- (16) T. Sherman, *J. Soc. Cosmet. Chem.*, **17**, 439 (1966).
- (17) T. Sherman, *J. Colloid Interface Sci.*, **24**, 107 (1967).
- (18) T. Sherman, "Emulsion Sciences," Academic, New York, N.Y., 1968.
- (19) J. D. Ferry, "Viscoelastic Properties of Polymers," Wiley, New York, N.Y., 1970.
- (20) J. R. Van Wazer, J. W. Lyons, K. Y. Kim, and R. E. Colwell, "Viscosity and Flow Measurements—A Laboratory Handbook of Rheology," Interscience, New York, N.Y., 1963.
- (21) G. B. Thurston, *Biophys. J.*, **12**, 1205 (1972).
- (22) D. R. Bland, "The Theory of Linear Viscoelasticity," Pergamon Press, Oxford, England, 1960.
- (23) T. Alfred, Jr., and E. F. Gurnee, in "Rheology, Theory and Applications," E. R. Eirich, Ed., Academic, New York, N.Y., 1956, chap. 10.
- (24) R. Cerf, *J. Phys. Radium*, **13**, 458 (1952).
- (25) H. A. Scheraga, *J. Chem. Phys.*, **23**, 1526 (1955).
- (26) B. H. Zimm, *ibid.*, **24**, 269 (1956).
- (27) R. Cerf, *J. Phys. Radium*, **19**, 122 (1958).
- (28) R. Cerf, *J. Polym. Sci.*, **23**, 125 (1957).
- (29) A. Peterlin, *Kolloid-Z.*, **209**, 181 (1966).
- (30) A. Peterlin, *J. Polym. Phys.*, **5**, 179 (1967).
- (31) G. B. Thurston and A. Peterlin, *J. Chem. Phys.*, **46**, 4881 (1967).
- (32) R. B. Bird, *Annu. Rev. Fluid Mech.*, **8**, 13 (1976).
- (33) W. W. Graessley, *Adv. Polym. Sci.*, **16** (§8.2), 1 (1974).
- (34) A. Dyson, *Trans. R. Soc. London*, **258**, 529 (1965).
- (35) W. Philippoff, *J. Appl. Phys.*, **36**, 3033 (1965).
- (36) W. E. Stewart and J. P. Sorensen, *Trans. Soc. Rheol.*, **16**, 1 (1972).
- (37) R. B. Bird, H. R. Warner, and D. C. Evans, *Adv. Polym. Sci.*, **8**, 1 (1971).
- (38) R. I. Tanner and J. M. Simmons, *Chem. Eng. Sci.*, **22**, 1803 (1967).
- (39) R. I. Tanner, *AIChE J.*, **15**, 177 (1969).
- (40) J. Lamb, "Viscoelastic Behavior and the Lubricating Properties of Liquids," Symposium on Rheology, ASME Applied Mechanics and Fluids Engineering Conference, Washington, D.C., June 1965.
- (41) M. C. Williams, *AIChE J.*, **12**, 1064 (1966).
- (42) G. B. Thurston, *J. Acoust. Soc. Am.*, **32**, 210 (1960).
- (43) G. B. Thurston, *Biorheology*, **13**, 191 (1976).
- (44) G. B. Thurston, *Microvasc. Res.*, **11**, 133 (1976).
- (45) J. B. Segur and H. E. Oberstar, *Ind. Eng. Chem.*, **43**, 2117 (1951).

### ACKNOWLEDGMENTS

The authors thank Ms. Gloria Querijero for assistance in preparing samples and for determinations of steady shear values.